Building the red sequence through gas-rich major mergers

Vivienne Wild[1], C. Jakob Walcher[2] & Peter H. Johansson[3]

[1] Institut d'Astrophysique de Paris, CNRS, Université Pierre & Marie Curie,
UMR 7095, 98bis bd Arago, 75014 Paris, France. email: `wild@iap.fr`

[2] European Space Agency, Keplerlaan 1, 2200AG Noordwijk, The Netherlands

[3] Universitäts-Sternwarte München, Scheinerstr. 1, D-81679 München, Germany

Abstract. Understanding the details of how the red sequence is built is a key question in galaxy evolution. What are the relative roles of gas-rich vs. dry mergers, major vs. minor mergers or galaxy mergers vs. gas accretion? In a recent paper (Wild *et al.* 2009), we compare hydrodynamic simulations with observations to show how gas-rich major mergers result in galaxies with strong post-starburst spectral features, a population of galaxies easily identified in the real Universe using optical spectra. Using spectra from the VVDS deep survey with $<z> = 0.7$, and a principal component analysis technique to provide indices with high enough SNR, we find that 40% of the mass flux onto the red-sequence could enter through a strong post-starburst phase, and thus through gas-rich major mergers. The deeper samples provided by next generation galaxy redshift surveys will allow us to observe the primary physical processes responsible for the shut-down in starformation and build-up of the red sequence.

Keywords. galaxies: stellar content, starburst, interactions; surveys

1. Introduction

Recent observations have revealed that since a redshift of around unity the total mass of stars living in red sequence galaxies has increased by a factor of two (e.g. Bell *et al.* 2004). At the same time, the stellar mass density of the blue sequence has remained almost constant. The interpretation is that some blue galaxies migrate onto the red sequence after the quenching of their star formation, whilst the remainder continue to form new stars (e.g. Faber *et al.* 2007).

Arnouts *et al.* (2007) measured the net mass flux which has taken place from the blue sequence to the red sequence. This amounts to $9.8 \times 10^{-3} M_\odot/\mathrm{yr}/\mathrm{Mpc}^3$, or about $1.4 \times 10^4 \, M_\odot/\mathrm{yr}$ in the VIMOS VLT DEEP Survey (VVDS) volume. Recent star formation history can be used as a tool to identify galaxies as they enter the red sequence. For typical observable times of post-starburst features in VVDS optical galaxy spectra of $\sim 0.35 - 0.6 \, \mathrm{Gyr}$, this could comprise, for example, a few tens of galaxies of stellar mass $\log(M/M_\odot) = 10.5$ in the VVDS survey. In these proceedings I will summarise the work presented in detail in Wild *et al.* (2009) and ask whether observations of post-starburst galaxies are consistent with the growth of the red-sequence being caused by gas-rich major mergers.

2. Post-starbursts in major merger simulations

Alongside toy models of star formation histories, modern advanced simulations afford a new means of interpretation of observational results. Smoothed particle hydrodynamic (SPH) simulations of galaxy mergers are now carried out routinely by several groups,
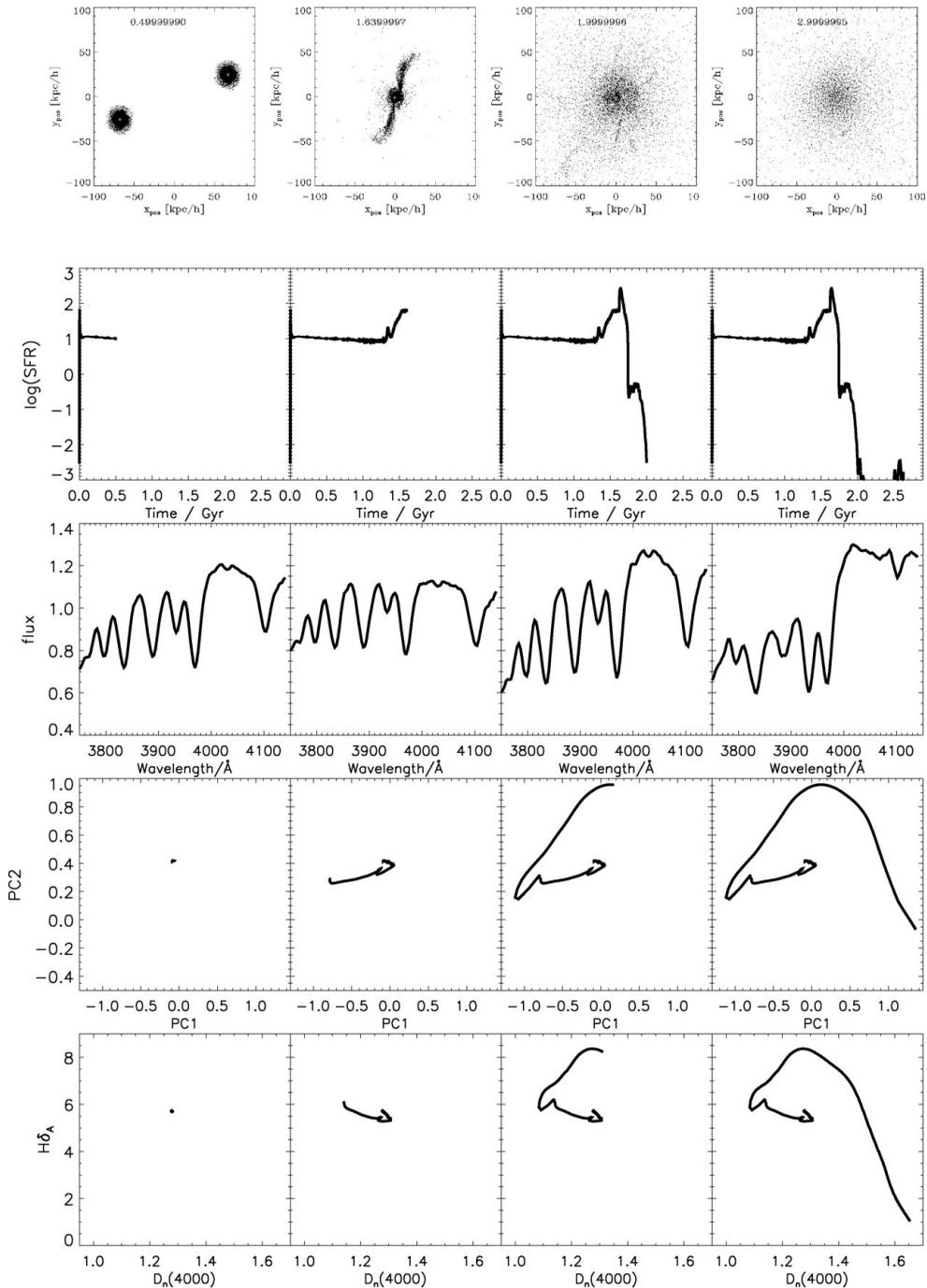
Figure 1. From left to right snapshots of a hydrodynamic simulation of a major galaxy merger, at 0.5 Gyr (initial starforming disks), 1.64 Gyr (peak of starburst), 2 Gyr (peak of post-starburst features) and 3 Gyr (remnant) after the start of the simulation. From top to bottom: the $x - y$ positions of gas particles and black holes (purple points); trace of combined star-formation rate of both galaxies; the optical continuum spectrum in 4000Å break region (note that emission lines, have not been plotted to improve clarity); the trace of PCA derived indices that describe the strength of the 4000Å break and the Balmer absorption lines; the trace of two indices used traditionally to infer the recent star formation history of galaxies.

and while we await new advances in combining radiative transfer with SPH merger and cosmological simulations (Jonsson *et al.* 2006), simple comparisons can be already be made. For a suite of 79 merger simulations presented in Johansson *et al.* (2009) we used standard stellar population synthesis, dust attenuation law and Balmer emission predictions to recreate the "observed" spectra of the merging galaxies.

In Figure 1 we present four snapshots in time of one particular merger simulation, chosen to illustrate the peak differences in the optical spectral features. One traditional index used for identifying post-starburst galaxies, the Balmer $H\delta_A$ absorption line is compared with our new method which combines all 5 Balmer lines visible in the 4000Å break region, together with the changing shape of the continuum using a Principal Component Analysis based on the method described in Wild *et al.* (2007). As the merger commences, the sudden presence of hot O and B stars cause a rapid increase in the blue-UV continuum causing a decrease in the measured 4000Å break strength. Within $\sim$0.5 Gyr a combination of exhaustion of the gas supply and disruption and expulsion of gas by the energy of many supernovae causes the star formation rate to decline rapidly. The loss of the contribution of short-lived O and B stars to the integrated spectrum, and the dominance of slightly cooler and longer-lived A and F stars, cause the strong Balmer absorption features of the post-starburst phase. In this particular simulation, QSO feedback is included, causing the further shut-down of star formation. However, the presence or absence of QSO feedback makes very little difference to the strength of the post-starburst features, or the observational lifetime of the post-starburst phase.

From our analysis of both toy-models and merger simulations, we find that gas-rich spiral mergers can lead to galaxies with strong Balmer absorption features before the galaxy enters the red sequence. However, the timescale of the decay in star formation must be short ($< 10^8$yrs) and the burst mass fraction must be large ($> 5 - 10\%$) for post-starbursts to be observed using VVDS spectra. The strongest starbursts visible in the VVDS dataset are detectable for 0.6 Gyr in the post-starburst phase.

3. VVDS post-starburst galaxies

The VVDS is a deep spectroscopic redshift survey, targeting objects with apparent magnitudes in the range of $17.5 < I_{AB} < 24$. The survey is unique for high-redshift galaxy surveys in having applied no further colour cuts to minimize contamination from stars, yielding a particularly simple selection function. The spectra have a resolution (R) of 227 and a useful observed frame wavelength range, for our purposes, of 5500-8500Å. In this work we select 1246 galaxies with $0.5 < z < 1.0$, $I_{AB} < 23$ and per-pixel S/N > 6.

In the left panel of Figure 2 the distribution of spectral indices "PC1" (equivalent to 4000Å break strength) and "PC2" (excess Balmer absorption) is shown. The majority of galaxies form a well defined sequence from red and dead galaxies with strong 4000Å breaks to blue, star-forming galaxies with weaker breaks. A tail of starburst galaxies exists to the bottom left, where there has been a sharp increase in the galaxy's star formation rate over a timescale that is short ($\sim 10^8$yrs) in comparison to the age of the galaxy (thus distinguishing them from more ordinary "starforming" galaxies). The orange crosses indicate the galaxies with strong Balmer absorption lines, indicative of a recent sharp shut-down in starformation. The encircled points indicate those galaxies with no ongoing star formation, as measured from a fit to their multi-wavelength spectral energy distribution (Walcher *et al.* 2008). For comparison to other E+A samples, these galaxies also have no visible [OII]λ3727,3730 emission, we note that they have a tendency to be older than the star-forming post-starbursts. In the right hand panel of Figure 2, the mass distribution of the different types of galaxies is plotted, both before and after
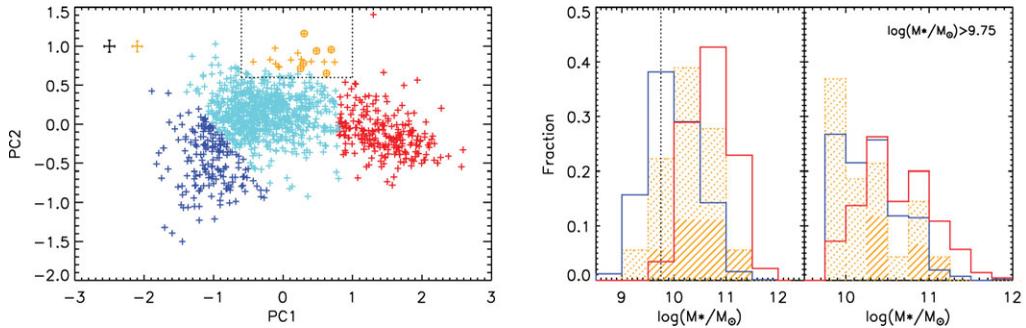
Figure 2. *Left:* the distribution of PC1 vs. PC2 for all galaxies in our VVDS sample. PC1 is equivalent to the well-known index $D_n 4000$, PC2 represents the excess (or lack) of Balmer absorption. For illustration purposes, the sample has been split into quiescent (right, red), star forming (center, cyan), star-bursting (bottom left, blue) and PSB (in box, orange) classes. Those PSB galaxies with SSFR$< 10^{-11}$/yr are circled. *Right:* the mass distribution of galaxies, before (left) and after (right) correction for survey incompleteness effects. Histograms are normalised to unity. The orange dot-filled histograms are all PSB galaxies, the line-filled histograms are the subset with no ongoing residual star formation. The vertical dotted line indicates our PSB mass completeness limit.

correction for survey incompleteness effects. The post-starburst sample is complete above a mass limit of $5.6 \times 10^9 M_\odot$ and the non-starforming post-starbursts have masses in the same range as red-sequence galaxies at this redshift.

4. The mass flux onto the red sequence

By summing the total mass of post-starburst galaxies and using our knowledge from simulations to estimate how long they will be visible for, we can measure the mass flux from the blue to the red-sequence that passes through a post-starburst phase. In this calculation, we include only the five galaxies which have completely stopped star-formation and therefore we argue are certain to be heading for the red-sequence.

$$\dot{\rho}_{\mathrm{B \to R, PSB}} = \frac{\mathrm{M_{B \to R, PSB}}}{\mathrm{Vol} \times \mathrm{t_{PSB}}} = 0.0038 \mathrm{M_\odot/Mpc^3/yr} \qquad (4.1)$$

Comparing to the total mass flux from the blue to the red sequence measured by Arnouts *et al.* (2007), this represents $38^{+4}_{-11}\%$ of the build-up of mass onto the red sequence. We therefore conclude that post-starburst galaxies are more than an interesting curiosity, and while this result may be regarded as preliminary as it relies on only 5 galaxies, our study shows how deeper spectroscopic surveys will reveal directly the physical processes responsible for the shut-down in star-formation.

References

Arnouts S., Walcher C. J., Fèvre O. L., *et al.* 2007, A&A, 476, 137
Bell E. F., Wolf C., Meisenheimer K., *et al.* 2004, ApJ, 608, 752
Faber S. M., Willmer C. N. A., Wolf C., *et al.* 2007, ApJ, 665, 265
Johansson P. H., Naab T., & Burkert A., 2009, ApJ, 690, 802
Jonsson P., Cox T. J., Primack J. R., & Somerville R. S., 2006, ApJ, 637, 255
Walcher C. J., Lamareille F., Vergani D., *et al.* 2008, A&A, 491, 713
Wild V., Kauffmann G., Heckman T., *et al.* 2007, MNRAS, 381, 543
Wild V., Walcher C. J., Johansson P. H., *et al.*, 2009, MNRAS, 395, 144